

Conformers of Nonionized Proline. Matrix-Isolation Infrared and Post-Hartree–Fock ab Initio Study

S. G. Stepanian,^{†,‡} I. D. Reva,[‡] E. D. Radchenko,[‡] and L. Adamowicz^{*,†}

Department of Chemistry, University of Arizona, Tucson, Arizona 85721, U.S.A., and Institute for Low-Temperature Physics and Engineering, National Academy of Sciences of Ukraine, 47 Lenin Avenue, Kharkov 61164, Ukraine

Received: May 4, 2001; In Final Form: August 27, 2001

Matrix-isolation IR spectroscopy and ab initio calculations performed at the DFT, MP2, MP4, and CCSD(T) levels of theory were employed to investigate the conformational topology of the nonionized amino acid proline and its deuterated derivative, *N,O*-dideuteroproline (proline-*d*₂). In the calculations, equilibrium structures of 15 low-energy proline conformers were obtained using the DFT/B3LYP/aug-cc-pVDZ and MP2/aug-cc-pVDZ methods. The harmonic frequencies and IR intensities of the conformers were calculated for the DFT geometries, and these data was used to account for the zero-point vibration energy correction and to assist the analysis of the experimental matrix-isolation IR spectra. Two proline conformers were found to be present in the Ar matrix. They are the lowest energy conformer with a N···H–O H bond (conformer **IIa**) and the second conformer with a NH···O=C H bond (conformer **Ia**). We found that the DFT/B3LYP and MP2 methods are not capable of predicting the relative energies of the proline conformers with a quantitative accuracy. Both methods provide the energy difference between the **IIa** and **Ia** conformers of 7–8 kJ mol⁻¹, thus suggesting that only conformer **IIa** should be present in the matrix. However, strong bands due to the two conformers are observed in the experimental spectra and their intensities indicate approximately equal presence of the two systems in the matrix. To explain the discrepancy between the MP2 and DFT results and the experiment, calculations were performed at the CCSD(T) level of theory. The relative energy difference obtained at this level of 3.9 kJ mol⁻¹ better agrees with the experiment because it is less than *kT* at the matrix preparation temperature. The observed low-frequency shift of the OH stretching vibration due to the intramolecular N···H–O H bond in the proline conformer **IIa** of 534 cm⁻¹ is much larger than the ones found for other amino acids (340–360 cm⁻¹). It demonstrates that the intramolecular H bonding in proline is much stronger than in other amino acids.

1. Introduction

The conformational behavior of the natural amino acids is of special interest because it determines the functional specificity of proteins and polypeptides. Proline is an exception among 20 natural amino acids. Its nitrogen atom is bonded to the aliphatic side chain forming the five-member pyrrolidine ring. This should significantly constrain the conformational flexibility of proline. At the same time the presence of the flexible ring adds new structural features that are only specific to proline. Perhaps this unique structural feature of the proline side chain is responsible for the specific function of proline in the β - and γ -turns of polypeptide chains.^{1–5}

The structural investigation of the solid proline⁶ revealed its zwitterionic (bipolar) structure: NH₂⁺–CH(R)–COO⁻, but this form does not occur in the polypeptide chain. The form that appears there is similar to the neutral (nonzwitterionic) form of amino acids. The simplest amino acids, glycine and alanine, were found to exist in the neutral form in the gas phase.^{7–17}

Experimental studies of the gas-phase amino acids are difficult due to low thermal stability of these compounds. They usually

decompose before melting. The microwave,^{7–9,11–13,15} low-resolution photoelectron spectroscopy^{16,17} and electron diffraction^{10,14} studies allowed identification of two glycine and two alanine conformers. These conformers are stabilized by either NH···O=C or N···H–O intramolecular H bond.

Recently we applied the matrix-isolation IR spectroscopy combined with ab initio calculations to investigate conformations of gas-phase amino acids frozen in low temperature inert gas matrices.^{18–21} In these studies we used a low temperature quartz microbalance to measure the gaseous flows of the amino acids during the matrix sample deposition. This allowed us to determine the optimal evaporation temperatures, which was high enough to yield matrix samples with sufficient concentration of the studied compound but still sufficiently low to prevent decomposition of the compound. We demonstrated that IR spectroscopy is a suitable tool to study amino acids due to its high sensitivity to the intramolecular H bonding. In the studies we identified three glycine,^{18,19} two alanine,²⁰ and three valine²¹ conformers. In the studies we applied the DFT/B3LYP and MP2 quantum-mechanical methods to calculate the structures of the conformers and to predict their IR spectral parameters. We found that the DFT/B3LYP method provides the most accurate frequencies for the different conformers of the studied amino acids. We also determined optimal factors for scaling the calculated frequencies to match experimental frequencies for

* Corresponding author. Fax: 520-621-8407. E-mail: ludwik@u.arizona.edu.

[†] University of Arizona.

[‡] National Academy of Sciences of Ukraine.

several basis sets typically used in IR frequency calculations of systems with intramolecular H bond.¹⁹ The cc-pVDZ atomic-orbital basis set augmented with diffuse s and p shells on hydrogen atoms and with s, p, and d diffuse shells on heavy atoms (the aug-cc-pVDZ basis set) was found to be a very good basis in predicting the IR spectra of neutral amino acid conformers. As expected the presence of the diffuse atomic orbitals in the basis is critical to generate highly accurate vibrational frequencies of molecules with intramolecular H bonding in the calculations. The equilibrium structures of the amino acid conformers obtained at the DFT/B3LYP and MP2 levels of theory are in good agreement with available experimental data.^{7–15}

The conformational structure of proline was a subject of several theoretical studies.^{22–25} Ramek et al.²⁴ located 10 glycine conformers at the HF/6-311++G** level of theory, and more recently, Csaszar and Perczel²⁵ located 12 proline conformers at the B3LYP/6-311++G** level. The stability order of the proline conformers was found to strongly depend on the level of theory used in the calculations.

The only experimental information about the gas-phase proline was obtained in our earlier study.²⁶ We demonstrated that proline molecules in the gas phase exist in the neutral form. This conclusion was derived on the basis of the presence of a strong absorption in the IR spectral region of the C=O stretching vibration. But the conformational gas-phase behavior of the neutral proline has not been known. Thus in the present work we have undertaken a detailed investigation of the conformational structure of proline using the matrix-isolation technique coupled with high-level ab initio calculations and we present evidence of the existence of two proline conformers with different intramolecular H bonds in the matrix. We also demonstrate that, unlike in other amino acids, the DFT/B3LYP and MP2 methods are not capable of predicting correct relative stabilities of the proline conformers. The stabilities obtained with those methods disagree both with the experimental data and with the results obtained at the CCSD and CCSD(T) levels of theory.

2. Experimental Details

The updated SPECORD IR 75 spectrometer was used to register the IR spectra of the matrix isolated proline and *N,O*-dideuterioproline (proline-*d*₂) in the range 4000–400 cm⁻¹. The resolution of the instrument in the range 4000–2500 cm⁻¹ was 3 cm⁻¹, and in the range 2500–400 cm⁻¹ was 1 cm⁻¹. The spectrometer was sealed and blown through with dry nitrogen during the experiment to exclude any influence of the atmospheric H₂O and CO₂.

The matrix samples were prepared by a simultaneous deposition of the substance and the matrix gas onto a cooled CsI substrate. The matrix gas was 99.99% Ar. The substrate temperature was 14 K during matrix preparation. The compound studied was evaporated from the Knudsen cell at 152 °C. This temperature was found to be high enough to yield samples with sufficient concentration of the compound, but still sufficiently low to prevent its decomposition. The fill-up helium cryostat used in the matrix-isolation IR experiments was described elsewhere.²⁷ The low-temperature quartz microbalance was used to measure the gaseous flows of the studied compounds and of the matrix gas. By adjusting these flows we were able to prevent an appearance of autoassociates in the spectrum. The relative concentrations of proline and proline-*d*₂ to argon in the matrix equaled 1:1150 and 1:750, respectively.

The IR spectrum of proline recorded immediately after sample deposition is presented in Figure 1. It shows no bands of any

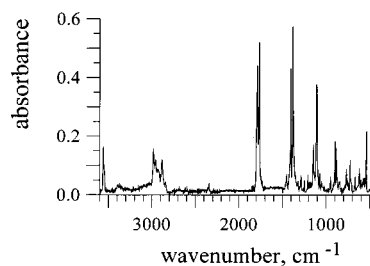


Figure 1. Matrix-isolation IR spectrum of proline recorded for a sample deposited at 14 K. The matrix ratio is 1:1150.

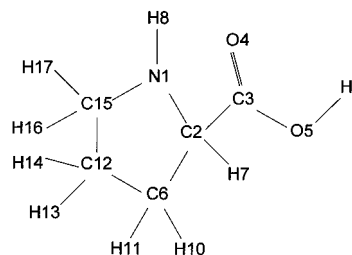


Figure 2. Atom numbering for proline.

decomposition products. Only a few weak bands corresponding to trace amounts of CO₂ and H₂O appear in the spectra. These bands are most probably due to CO₂ and H₂O adsorbed on the surface of the solid compound used in the experiment.

3. Theoretical Methods

The conformational structure of the proline molecule (Figure 2) may be characterized with four torsion parameters. They are (i) the O4C3O5H9 torsion, which may have values around 0° and 180° corresponding to the *syn*- and *anti*-periplanar orientations of the O–H and C=O groups, (ii) the N1C2C3O4 torsion, which describes the orientation of the carboxyl with respect to the ring, (iii) the H8N1C2C6 torsion, which describes the orientation of the N–H bond with respect to the ring, and (iv) the N1C2C6C12 torsion, which is the ring pucker angle.

The set of initial structures with all possible combinations of the torsions listed above were fully optimized using the DFT method. These calculations were carried out with the three-parameter density functional, usually abbreviated as B3LYP, which includes Becke's gradient exchange correction,²⁸ the Lee, Yang, Parr correlation functional²⁹ and the Vosko, Wilk, and Nusair correlation functional.³⁰ The standard aug-cc-pVDZ basis set was used in the calculations, and 15 unique proline conformers were found in the calculations.

To determine whether the minima found on the potential energy surface (PES) of proline correspond to true equilibrium configurations, we performed harmonic frequency calculations at all the DFT/B3LYP/aug-cc-pVDZ equilibrium structures found in the calculations. No imaginary frequencies were obtained, indicating that the structures found correspond to true PES minima. The harmonic frequencies were also used to account for the zero-point vibrational energy (ZPVE) corrections to the relative energies of the conformers. The MP2/aug-cc-pVDZ single point energy calculations were also done for all conformers.

Next, the geometries of four lowest energy proline conformers were reoptimized at the MP2/aug-cc-pVDZ level of theory. This was followed by single point energy calculations at the MP4-(SDTQ)/aug-cc-pVDZ^{31,32} and CCSD(T)/aug-cc-pVDZ^{33–36} levels. These calculations were done to obtain more accurate energy differences between the conformers. All calculations in this work

TABLE 1: Characteristic Frequencies (cm^{-1}) of the OH Stretching Vibrations of Conformers I and II Observed in the IR Spectra of the Matrix Isolated Aminoacids

amino acid	conformer I	conformer II	ref
glycine	3560	3200	19
alanine	3560	3193	20
valine	3561	3183	21
leucine	3565	3193	40
isoleucine	3557	3187	40
norvaline	3559	3214	40

were done on the SGI Origin 2000 supercomputer using the Gaussian 98³⁷ quantum-mechanical program.

4. Results and Discussion

Matrix IR Spectra of Proline. In our recent studies^{19–21} we observed two different types of amino acid conformers: one with the $\text{N-H}\cdots\text{O}$ intramolecular H bond (denoted as **I**) and the other with the $\text{N}\cdots\text{H-O}$ H bond (denoted as **II**). We also established some characteristic IR spectral features of these types of conformers that may be used in their identification using the IR spectroscopy.²¹ The most important of these features are strong narrow bands of the OH stretching vibrations of the type-**I** conformer at 3560 cm^{-1} and wide bands of the type-**II** conformer that are observed near 3200 cm^{-1} and that also correspond to the OH stretching vibrations. The low-frequency shift of the OH stretch of 360 cm^{-1} is due to the intramolecular $\text{N}\cdots\text{H-O}$ H bond in conformers **II**. In Table 1 we summarized the experimental frequencies of the OH stretches observed for a set of natural amino acids studied with the matrix-isolation technique. As seen from Table 1, the OH stretching vibration frequencies of conformers **I** and **II** are highly characteristic and may serve as the most useful tool to determine the conformational structure of the amino acids.

Therefore it seems reasonable to start the study of the proline conformational behavior with the analysis of the OH stretching vibration region, which is presented in Figure 3. The numbering scheme of the proline conformers used in this work is shown in Figure 4. As seen in the spectrum, the highest frequency band is observed at 3559 cm^{-1} and can be assigned to the OH stretching vibration of conformer **I**. The presence of this band proves the presence in the matrix of at least one proline conformer with the OH group not involved in the intramolecular H bonding. Another feature of the high-frequency spectral region is the absence of absorption near 3200 cm^{-1} . This may be evidence of absence in the matrix of the type-**II** proline conformer with an $\text{N}\cdots\text{H-O}$ intramolecular H bond.

Another vibration that is very sensitive to differences in the intramolecular H bonding in the amino acid conformers is the stretching vibration of the C=O group. Very strong bands of this vibration are usually observed in the $1820\text{--}1750\text{ cm}^{-1}$ region of the matrix spectrum. This region for proline is presented in Figure 3. Two strong bands split by 23 cm^{-1} with approximately equal integral intensities are observed in this region. The splitting should not be attributed to associations of proline molecules. As we demonstrated before,³⁸ the intermolecular interaction of the carboxyl group causes a stronger down frequency shift of the C=O stretch to $1720\text{--}1690\text{ cm}^{-1}$. Moreover at the 1:1150 matrix ratio only 2–3% of the proline molecules form dimers in the matrix.³⁹ The presence of the two bands in this region may be due to the different matrix structure surrounding the proline guest molecules, i.e., due to the so-called matrix splitting. One of the conventional methods to recognize a matrix splitting is the matrix annealing. In the case of matrix splitting a strong redistribution of the intensities of

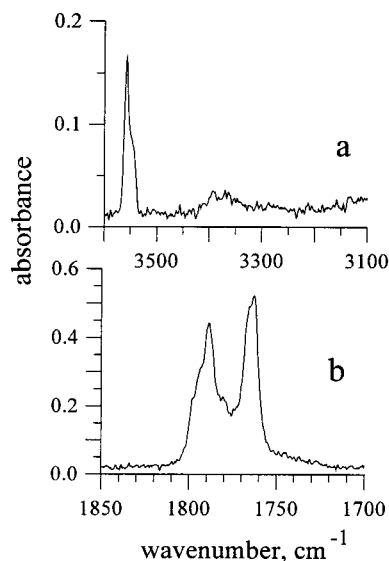


Figure 3. O–H stretching (a) and C=O stretching (b) vibration regions of the IR spectrum of proline.

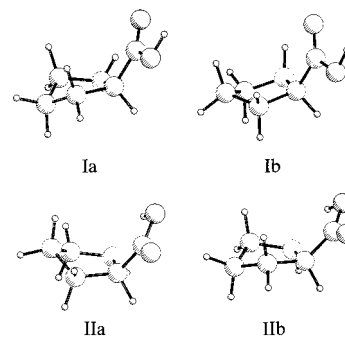


Figure 4. Lowest energy conformers of neutral proline.

the split bands is usually observed. However, the comparison of the proline spectra recorded before and after annealing does not reveal any changes of the band intensities. Therefore the bands at 1789 and 1766 cm^{-1} should not be attributed to matrix splitting but they should be due to two different proline conformers.

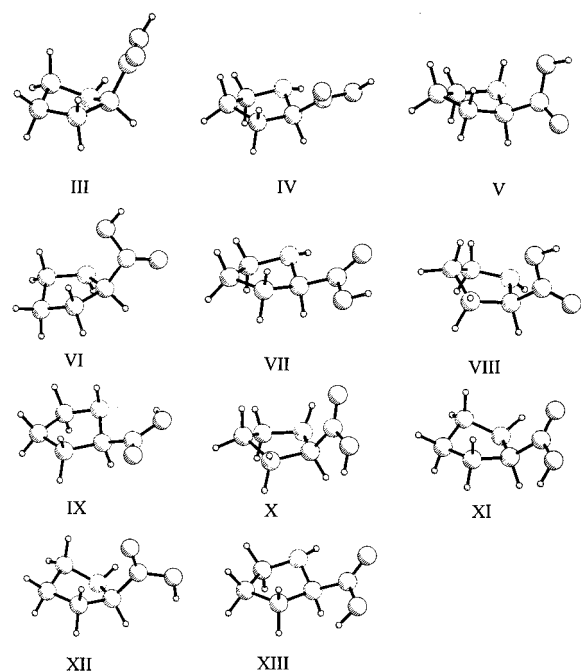
The main conclusions of the above analysis are as follows: we observe in the matrix at least two proline conformers, both with OH bonds that are not involved in intramolecular H bonding; these conformers should have almost identical frequencies of the OH stretching vibrations and different frequencies of the C=O stretching vibrations. A support for these conclusions is provided by our previous works on two amino acids, glycine¹⁹ and valine,²¹ where we also observed such conformer pairs. The two conformers within each pair were only different in terms of which oxygen atom interacts with the N-H bond. To provide further validation of our assignment for proline, we turned to calculations. Their primary aim was to determine all possible proline conformers, simulate their IR spectra and identify the conformers that give rise to the spectral data. We should mention that, as we demonstrated earlier,¹⁹ only conformers with total energies not higher than $\sim 4\text{--}5\text{ kJ mol}^{-1}$ from the lowest energy conformer, may be present in the inert-gas matrixes. The results of the computational findings are presented in the next section.

Relative Stabilities and the Structure of the Proline Conformers. Totally, 15 proline conformers were found in the calculations performed at the DFT/B3LYP/aug-cc-pVDZ level of theory. Four lowest energy conformers are presented in Figure

TABLE 2: Energies (au), Relative Stabilities (ΔE , kJ mol⁻¹), Zero Point Vibrational Energies^a (ZPVE, au), and Relative Stabilities Including the Zero Point Vibrational Energy (ΔE_{total} , kJ mol⁻¹) of the Proline Conformers^b

	DFT/B3LYP				MP2		
	energy	ΔE	ZPVE	ΔE_{total}	energy	ΔE	ΔE_{total}
IIa	-401.219913	-6.4	0.141133	-4.7	-400.108465	-8.8	-7.1
IIb	-401.219203	-4.5	0.141049	-3.0	-400.107669	-6.2	-4.7
Ia	-401.217488	0.0	0.140467	0.0	-400.105096	0.0	0.0
Ib	-401.217179	0.8	0.140694	1.4	-400.105155	-0.2	0.4
III	-401.214816	7.0	0.140594	7.3	-400.102909	5.7	6.0
IV	-401.214685	7.4	0.140382	7.1	-400.101991	8.1	7.8
V	-401.214192	8.6	0.140617	9.0	-400.102080	7.9	8.3
VI	-401.213456	10.6	0.140607	11.0	-400.101550	9.3	8.7
VII	-401.214106	8.9	0.140276	8.4	-400.101340	9.9	9.4
VIII	-401.213340	10.9	0.140380	10.7	-400.101156	10.3	10.1
IX	-401.211824	14.9	0.141048	16.4	-400.100076	13.2	14.7
X	-401.209971	19.7	0.140373	19.5	-400.098156	18.2	18.0
XI	-401.210138	19.3	0.140222	18.7	-400.097925	18.8	18.2
XII	-401.206670	28.4	0.140420	28.3	-400.094665	27.4	27.3
XIII	-401.206174	29.7	0.140042	28.6	-400.093582	30.2	29.1

^a Zero point vibrational energies were scaled by applying the scaling factors 0.96 for the OH, NH, and CH stretching vibrations and 0.99 for all other vibrations. ^b Values are taken from the full optimization and frequency calculations of the conformers at the DFT/B3LYP/aug-cc-pVDZ level and from the single point calculations at the MP2/aug-cc-pVDZ//DFT/B3LYP/aug-cc-pVDZ level. All relative energies were calculated with respect to conformer **Ia**.

**Figure 5.** Proline conformers **III–XIII**. (The geometries of the conformers are available from the corresponding author.)

4 and the rest of the conformers are presented in Figure 5. We use the following notation for the proline conformers: the two lowest energy conformers with the N–H···O=C H bond are denoted as **Ia** and **Ib** and the two lowest energy conformers with the N···H–O H bond are denoted as **IIa** and **IIb**. The same notations were used for the amino acids studied earlier.^{19–21} Conformers **a** and **b** differ in the ring pucker. The rest of the proline conformers (**III–XIII**) are numbered according to their relative stabilities calculated at the MP2/aug-cc-pVDZ level for the DFT/B3LYP/aug-cc-pVDZ geometries with accounting for the ZPVE corrections. The total and relative energies of the proline conformers are presented in Table 2.

Surprisingly, the DFT calculations predicted conformers **IIa** and **IIb** to be more energetically favorable than conformers **Ia** and **Ib**. What is even more surprising, is the energy difference between conformers **IIa** and **Ia** is 6.4 kJ mol⁻¹. The energy

difference calculated at the MP2/aug-cc-pVDZ level for the DFT-optimized geometries is even larger, 8.8 kJ mol⁻¹ (7.1 kJ mol⁻¹ after accounting for the ZPVE). To verify this result, we reoptimized the four lowest energy proline conformers (**Ia**, **Ib**, **IIa**, and **IIb**) at the MP2/aug-cc-pVDZ level, but this only insignificantly changed the energy differences between conformers **Ia** and **IIa** (to 7.1 kJ mol⁻¹). In all cases the energy difference was larger than the empirical threshold of about 4–5 kJ mol⁻¹ mentioned above. This would mean that only bands of a conformer (or conformers) with the N···H–O H bond should be observed in the matrix spectra and this result would disagree with the observed data. This was an unexpected result since earlier we observed very good agreement of the experimental data with both DFT/B3LYP/aug-cc-pVDZ and MP2/aug-cc-pVDZ predicted relative stabilities of the amino acid conformers.

To clarify the problem, we performed single point energy calculations at the MP2/aug-cc-pVDZ geometries by employing higher levels of theory, MP4(SDTQ) and CCSD(T) with different basis sets. The results of the calculations are presented in Table 3. As seen, increasing the level of theory leads to a significant decrease of the energy gap between conformers **I** and **II**. The gap reduces to less than 4 kJ mol⁻¹ at the CCSD/6-31++G** and CCSD(T)/6-31++G** levels. The energy difference is now smaller than kT with T being the matrix deposition temperature. This result means that both types of conformers should be present in the matrix. This explains the presence in the IR spectrum of the band of conformer **Ia** at 3559 cm⁻¹, but it is still unclear why we did not observe a band near 3200 cm⁻¹ that is typical to the type-**II** amino acid conformer.

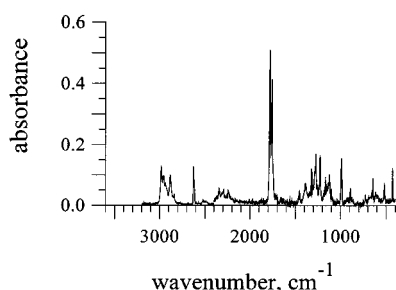
The answer to this question was found after the analysis of the calculated DFT/B3LYP/aug-cc-pVDZ frequencies of the OH stretching vibrations of conformers **Ia** and **IIa**. The frequency of the OH stretching vibration predicted for conformer **Ia** (3588 cm⁻¹) is similar to other amino acids, and it is in good agreement with the experimental data. But for conformer **IIa** the calculations predicted a much stronger (200 cm⁻¹) downshift of the OH-stretch frequency in comparison to the other amino acids.

The (observed frequency)/(unscaled predicted DFT frequency) ratio calculated for the OH stretch of the conformers of type-**II** using our previous data was ~ 0.92 for glycine,¹⁹

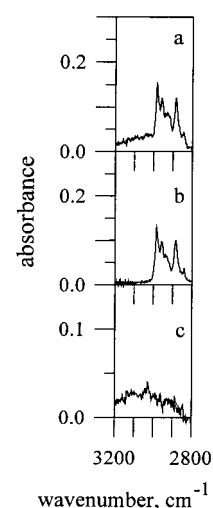
TABLE 3: Energies (au, First Row) and Relative Stabilities Including the Zero Point Vibrational Energy^a (kJ mol⁻¹, Second Row) of the Lower Energy Proline Conformers **Ia, **Ib**, **IIa**, and **IIb** Calculated at the Different Levels of Theory^b**

method	Ia	Ib	IIa	IIb
MP2/aug-cc-pVDZ//DFT/aug-cc-pVDZ	-400.105096 0.0	-400.105155 0.4	-400.108465 -7.1	-400.107467 -4.7
MP4(sdq)/aug-cc-pVDZ//DFT/aug-cc-pVDZ	-400.162532 0.0	-400.162376 1.0	-400.164702 -3.9	-400.163896 -2.0
MP2/aug-cc-pVDZ//MP2/aug-cc-pVDZ	-400.106019 0.0	-400.106108 0.4	-400.109327 -6.9	-400.108182 -4.1
MP4(sdq)/aug-cc-pVDZ//MP2/aug-cc-pVDZ	-400.163036 0.0	-400.162846 1.1	-400.164969 -3.3	-400.164153 -1.4
MP2/6-31++G**//MP2/aug-cc-pVDZ	-400.012051 0.0	-400.011651 1.6	-400.014982 -5.9	-400.013772 -3.0
MP4(sdq)/6-31++G**//MP2/aug-cc-pVDZ	-400.068594 0.0	-400.067975 2.2	-400.070187 -2.4	-400.069266 -0.2
MP4(sdtq)/6-31++G**//MP2/aug-cc-pVDZ	-400.116700 0.0	-400.117119 1.7	-400.119231 -4.8	-400.118300 -2.7
CCSD/6-31++G**//MP2/aug-cc-pVDZ	-400.066401 0.0	-400.065815 2.1	-400.067798 -1.9	-400.066940 0.1
CCSD(T)/6-31++G**//MP2/aug-cc-pVDZ	-400.110151 0.0	-400.109706 1.8	-400.112319 -3.9	-400.111457 -1.9

^a Zero point vibrational energies from the DFT/B3LYP/aug-cc-pVDZ calculation were scaled by applying the scaling factors 0.96 for the OH, NH, and CH stretching vibrations and 0.99 for all other vibrations. ^b All relative energies were calculated with respect to conformer **Ia**.

**Figure 6.** Matrix IR spectrum of proline-*d*₂ recorded for a sample deposited at 14 K. The matrix ratio is 1:750.

alanine,²⁰ and valine.²¹ We can use this value to scale the proline DFT frequency in question (i.e., the 3295 cm⁻¹ frequency of conformer **IIa**). The scaled value of this frequency is 3031 cm⁻¹. Thus the band of the OH stretching vibration of conformer **IIa** should appear in the region of the CH stretching vibrations (3050–2850 cm⁻¹). This explains why we did not observe this band near 3200 cm⁻¹. The two lowest energy proline conformers have 14 CH stretching vibrations and the bands of these vibrations conceal the band of the OH stretch. We carried out additional measurements of the matrix IR spectrum of the *N,O*-dideuterio-substituted proline, which is presented in Figure 6. In this spectrum we easily identify the OD stretching bands of both conformers: first band at 2626 cm⁻¹ assigned to conformer **Ia** (corresponding frequencies for glycine and alanine were 2631 and 2627 cm⁻¹, respectively) and the second band at 2295 cm⁻¹ assigned to conformer **IIa**. The latter band is downshifted with respect to the corresponding bands of other amino acids by ~100 cm⁻¹. We also used the IR spectrum of proline-*d*₂ to locate the band of the OH stretch of the nondeuterated proline conformer **IIa**. As mentioned, this band is expected to appear near 3000 cm⁻¹. For the region 3100–2900 cm⁻¹ we calculated the differential spectrum as (*proline absorbance*) minus (*proline-*d*₂ absorbance*). This allowed us to eliminate the bands of the CH stretches that are identical in both spectra and to identify the “missing” band of the proline conformer **IIa**. The differential spectrum is shown in Figure 7. As seen, a wide band is observed at 3025 cm⁻¹ and we assigned it to the OH stretching vibration of the proline conformer **IIa**. This band has a low peak and a high integral intensity and its shape is similar to the shapes of the corresponding bands of other amino acids.^{19–21}

**Figure 7.** Region of the CH stretching vibrations: (a) proline; (b) proline-*d*₂; (c) the differential spectrum.

As mentioned before, the structure optimizations of the proline conformers converged to two pairs of low-energy conformers, **Ia–Ib** and **IIa–IIb**. Different ring puckering distinguishes conformers **a** and **b**. Calculations predicted different frequencies for the conformers and all four conformers may be observed. But the relative energies are not the only parameters that determine the conformational composition of proline in the gas phase. Other important parameters are the energy barriers separating the conformers. If they are low, some conformers may interconvert to lower energy structures in the matrixes. Earlier we observed such interconversion of the glycine conformer **III** to conformer **I**, which occurred at the matrix temperature higher than 13 K (the energy barrier separated the glycine conformers **III** and **I** was 3.7 kJ mol⁻¹).¹⁹ For the lowest energy proline conformers we calculated the energy barriers at the DFT/B3LYP/aug-cc-pVDZ level. They are 0.8 and 3.3 kJ mol⁻¹ for the **Ib** → **Ia** and **IIb** → **IIa** interconversions, respectively, and are even smaller than the barrier in glycine. It indicates that conformers **Ib** and **IIb** isolated in the Ar matrix should easily interconvert to their lower energy counterparts. As a result, only two proline conformers, **Ia** and **IIa**, should be present in the matrix, and this is in agreement with the experimental spectra.

TABLE 4: Rotational Constants (MHz) and Dipole Moments (Debye) of the Lowest Energy Proline Conformers^a

conformer	A_c	B_c	C_c	μ
Ia	3834	1603	1318	1.71
Ib	3875	1555	1368	2.12
IIa	3792	1635	1294	6.26
IIb	3644	1684	1408	6.24

^a Values are taken from the full optimization of the conformers at the MP2/aug-cc-pVDZ level.

Thus, we found two proline conformers in the Ar matrixes, **Ia** and **IIa**. The spectral manifestations (bands of OH and OD stretching vibrations) of conformer **Ia** are similar to those of other amino acids. But the bands of the OH(OD) stretching vibrations in conformer **IIa** show unusually strong downshifts of approximately 200 and 100 cm^{-1} , respectively, comparing to the corresponding bands of glycine, alanine, and valine. The band splitting observed in the region of the C=O stretching vibrations is consistent with the splitting of the OH stretching vibration. The higher frequency band in the 1820–1750 cm^{-1} region is assigned to conformer **IIa**. The band of conformer **Ia** is downshifted due to the N–H \cdots O=C H bond interaction.

The presented data demonstrate that the N \cdots H–O H bond in proline is much stronger than in other amino acids studied. This results in additional stabilization of conformer **IIa** with respect to conformer **I** and makes the proline the only amino acid whose type-**II** conformer is the lowest energy form. This also results in a stronger downshift of frequency in the OH stretching vibration of conformer **IIa**. To determine whether the higher strength of the N \cdots H–O H bond in proline and in other amino acids correlates with lengths of the H bonds in these systems, we compared the amino acid geometries obtained at the MP2/aug-cc-pVDZ level of theory for the type-**II** conformers. The analysis showed that the length of the H bond in proline (1.827 Å) is indeed shorter than in other amino acids (1.905 Å in glycine, 1.893 Å in alanine, and 1.888 Å in valine).

Rotational constants, dipole moments, and structural parameters of the lowest energy proline conformers obtained at the MP2/aug-cc-pVDZ level of theory are collected in Tables 4 and 5. The rotational constants may be useful in searching for the neutral proline conformers with the microwave spectroscopy. One should notice that the dipole moments of the proline conformers **IIa** and **IIb** are much higher than ones of conformers **Ia** and **Ib**. This should produce for conformers **IIa** and **IIb** strong signals in the microwave spectra. The electron diffraction spectra of proline have not been obtained yet. The structural parameters of the proline conformers (Table 5) may assist the analysis of these spectra.

Assignment of the IR Spectra. The observed and simulated at the DFT/B3LYP/aug-cc-pVDZ level the IR spectra of proline and proline- d_2 are presented in Tables 6 and 7, respectively. The bands of the OH and C=O stretching vibrations were discussed above and here we briefly analyze only those proline vibrations that are sensitive to the different intramolecular H bonding.

In addition to the OH stretches, in the higher frequency region of the spectra we also observe weak bands assigned to the NH (proline) and ND (proline- d_2) stretching vibrations. These vibrations are split in both spectra, by 24 cm^{-1} for proline and by 20 cm^{-1} for proline- d_2 . The higher components are assigned to conformer **IIa**. The bands of conformer **Ia** are downshifted due to the N–H \cdots O=C H bonding. There is a larger difference between the conformational splitting of the NH(ND) and OH(OD) stretching vibrations. The bands of the OH(OD) stretches are split by 534 cm^{-1} in the proline spectrum and by 331 cm^{-1}

TABLE 5: Optimized Geometry Parameters of the Lowest Energy Proline Conformers Obtained in the MP2/Aug-cc-pVDZ Calculations

	Ia	Ib	IIa	IIb
N1–C2	1.469	1.477	1.491	1.490
C2–C3	1.521	1.517	1.541	1.535
C3–O4	1.222	1.222	1.220	1.219
C3–O5	1.366	1.364	1.350	1.352
C2–C6	1.565	1.563	1.543	1.560
C2–H7	1.103	1.102	1.101	1.101
N1–H8	1.022	1.023	1.018	1.020
O5–H9	0.974	0.974	0.996	0.992
C6–H10	1.101	1.100	1.099	1.101
C6–H11	1.099	1.102	1.102	1.098
C6–C12	1.544	1.537	1.538	1.541
C12–H13	1.101	1.101	1.100	1.103
C12–H14	1.100	1.103	1.103	1.101
C12–C15	1.531	1.536	1.534	1.536
C15–H16	1.100	1.104	1.105	1.100
C15–H17	1.109	1.100	1.100	1.104
N1–C2–C3	112.8	110.9	109.6	109.8
C2–C3–O4	125.9	125.7	122.7	122.9
C2–C3–O5	111.1	111.3	113.6	113.7
C3–C2–C6	110.2	109.8	110.5	111.4
C3–C2–H7	107.0	107.5	106.9	106.6
C2–N1–H8	109.7	106.8	111.3	109.4
C3–O5–H9	106.1	106.0	102.4	103.2
C2–C6–H10	110.1	112.3	111.6	109.6
C2–C6–H11	111.5	109.0	109.8	111.7
C2–C6–C12	103.9	102.7	102.0	103.7
C6–C12–H13	110.5	112.8	113.4	110.7
C6–C12–H14	112.4	110.4	110.2	112.7
C6–C12–C15	102.2	101.0	102.0	102.0
C12–C15–H16	113.5	110.0	109.9	114.8
C12–C15–H17	110.2	114.1	113.4	110.2
N1–C2–C3–O4	5.0	15.6	–182.3	–187.8
N1–C2–C3–O5	–174.9	194.5	–2.0	–7.8
O4–C3–C2–C6	–112.4	257.8	61.6	53.2
O4–C3–C2–H7	126.8	137.7	–60.8	–68.7
C3–C2–N1–H8	26.0	–4.3	120.3	135.2
C2–C3–O5–H9	–179.7	181.8	–0.1	0.4
C3–C2–C6–H10	5.1	–27.2	–31.6	13.3
C3–C2–C6–H11	–114.1	–147.0	–152.4	–105.8
C3–C2–C6–C12	98.6	96.3	91.0	101.3
C2–C6–C12–H13	88.9	159.5	162.4	85.5
C2–C6–C12–H14	–149.1	281.5	284.3	–152.8
C2–C6–C12–C15	–27.4	37.8	41.3	–31.0
C6–C12–C15–H16	161.5	78.2	78.9	161.7
C6–C12–C15–H17	–76.1	199.8	200.7	–75.6

in the proline- d_2 spectrum. It confirms that in the proline conformers the N \cdots H–O H bonding is much stronger than the N–H \cdots O=C H bonding.

Other vibrations that are worth noticing are the OH bending and torsion vibrations (Tables 6 and 7). The H bonding in conformer **IIa** causes a higher frequency shift of these vibrations with respect to conformer **Ia** by 126 and 323 cm^{-1} , respectively. Again, these shifts are stronger than in the spectra of other amino acids. For example, the corresponding shifts of the OH bending and the torsion vibration in the glycine spectrum are 110 and 261 cm^{-1} .¹⁹ As seen in Tables 6 and 7, the calculated spectra of two proline conformers allows us to assign almost all observed bands. We analyzed the unassigned bands and determined that they certainly cannot be attributed to any other proline conformers. Thus these bands are most probably overtones or combined bands.

Relative Stabilities of the Amino Acid Conformers I and II. In our previous studies of the amino acid conformational structure we used the DFT/B3LYP and MP2 methods to predict the energies of the amino acids conformers and found that these methods produced the relative stabilities that are in good agreement with experimental results. But in this work we found

TABLE 6: Observed and Calculated (at the DFT/B3LYP/aug-cc-pVDZ level) IR Frequencies (cm⁻¹) and Intensities of Proline

observed ^a			calculated						observed ^a			calculated					
			proline Ia			proline IIa						proline Ia			proline IIa		
ν	A^b	I_{obs}^c	ν	I_{calc}^d	assignment ^e	ν	I_{calc}^d	assignment ^e	ν	A^b	I_{obs}^c	ν	I_{calc}^d	assignment ^e	ν	I_{calc}^d	assignment ^e
3559	0.16	2.69	3588	65.9	OH str				1105	0.35	2.94	1104	41.6	ring bend	1105	30.5	N1C2 str
3545	0.07								1072	0.06	0.26				1076	8.7	ring tor
3393	0.03	0.54				3413	65.9	NH str	1021	0.02	0.12	1049	1.9	C6C12 str	1045	2.0	C2C6 str
3369	0.02	0.50	3396	16.3	NH str				976	0.02	0.04	979	6.5	ring bend			
3025	0.03	5.20				3163	342.0	OH str	955	0.02	0.13	958	1.4	C6C12 str	952	5.7	ring bend
2984	0.12	2.10	2997	30.2	C6H str	3008	9.5	C6H str	950	0.05	0.23				950	11.6	C2C6 str
			2983	25.5	C15H str	2990	27.3	CH str	916	0.04	0.16				914	2.0	C6C12 str
2959	0.09	1.98	2952	51.0	C12H str	2961	34.7	CH str	907	0.04	0.17	904	1.0	ring bend			
2934	0.05	2.34	2935	17.7	C6H str	2948	28.1	CH str	899	0.12	0.97	922	0.2	C12C15 str	922	76.2	OH tor
						2935	14.4	CH str	896	0.15							
2916	0.06		2931	19.6	C12H str	2930	13.3	CH str	884	0.16	0.65				889	7.7	N1C2C3 bend
2885	0.11	2.28	2892	26.6	C2H str				876	0.06	0.42	873	14.1	ring bend	871	4.4	ring bend
2865	0.04	1.19				2884	64.4	CH str	853	0.04	0.35						
2846	0.03		2847	74.9	C15H str				844	0.04	0.31	849	7.8	N1C2C3O4 tor	847	7.0	O4C3C2C6 tor
1795	sh								822	0.02	0.06						
1789	0.45	7.22				1803	360.5	C=O str	782	0.03	0.46				793	3.8	C2C3 str
1781	sh								768	0.09	0.60	772	67.2	NH tor			
1766	0.52	6.03	1774	286.1	C=O str				751	0.05	0.18						
1488	0.02	0.05	1499	1.9	CH bend	1499	3.2	CH bend	726	0.11	0.85				724	15.1	N1C2C3O5 tor
			1476	2.4	CH bend	1476	5.9	CH bend	713	0.03	0.58	710	35.9	N1C2C3O4 tor			
1463	0.03	0.29	1461	4.1	NH bend	1464	5.2	CH bend	675	0.03	0.53						
1451	0.05	0.52	1446	10.3	CH bend				668	0.04							
1412	0.09	2.28				1425	213.2	OH bend	663	0.02							
1405	0.35	1.40							628	0.04	0.43	632	61.6	O4C3C2C6 tor			
1384	0.56	6.23				1407	151.6	NH bend	621	0.07	0.45				623	20.5	N1C2C3O4 tor
1381	0.46								603	0.04	0.24	605	20.7	C2C3O4 bend			
1364	0.08	0.83	1364	29.9	CH bend				597	0.03	0.21				582	5.9	C2C3O5 bend
1350	0.06	0.54				1349	6.5	CH bend	584	sh							
1330	0.03	0.10	1335	25.5	CH bend				576	0.05	0.52	579	19.3	OH tor			
1320	0.04	0.12	1318	0.5	CH bend	1324	2.1	CH bend	569	0.03	0.44						
1294	sh		1303	1.8	CH bend	1298	12.6	CH bend	564	0.05					570	6.9	ring bend
1286	0.06	0.32	1285	5.7	OH bend	1294	11.9	CH bend	560	0.04							
			1272	2.4	CH bend				551	0.04	0.17						
1247	0.06	0.10				1249	8.1	CH bend	546	0.11	1.26	549	44.3	OH tor			
			1230	0.4	N1C2C3 bend	1227	1.9	CH bend	541	0.21							
1210	0.04	0.25										411	15.1	C2C3O5 bend	461	2.3	C2C3O4 bend
1206	0.05					1205	17.5	C3O5 str				286	10.5	N1C2C3 bend	331	10.9	N1C2C3 bend
			1187	8.5	CH bend	1182	1.9	CH bend				259	0.9	ring tor	288	6.2	ring tor
1150	sh		1166	60.0	N1C2 str							194	0.5	ring tor	201	6.6	ring tor
			1160	6.3	CH bend							60	1.5	O4C3C2C6 tor	109	0.6	ring tor
1142	0.17	2.21				1148	27.5	C3O5 str				42	1.2	ring tor	55	2.3	O4C3C2C6 tor
1109	0.35	2.77	1120	221.7	C3O5 str												

^a Ar matrix deposited at 11 K. Sample-to-matrix ratio 1:1150. ^b A , experimental relative intensities. ^c I_{obs} , experimental relative integral intensities measured for the single bands or for the groups of merged bands. ^d I_{calc} , calculated intensities in km mol⁻¹. ^e Abbreviations: str, stretching; bend, bending; tor, torsion.

that the same methods failed for proline. They significantly overestimated the stability of the proline conformer **IIa** both with respect to the experiment and with respect to more accurate CCSD and CCSD(T) results. With this in mind one can question, how accurate were our previous energy results for glycine and alanine? To check this, we performed additional calculations of the relative energies of the glycine and alanine conformers **I** and **II** that were studied before with the MP2 and DFT methods.^{19,20} In these additional calculations we used the MP4-(SDQ) and CCSD levels of theory, the 6-31++G** basis set, and MP2/aug-cc-pVDZ equilibrium geometries. The results of the calculations are summarized in Table 8. The main conclusion that can be derived from the analysis of the data is as follow: the relative stabilities of the glycine and alanine conformers calculated at the MP2 level are very close to the MP4(SDQ) and CCSD ones. This is different from the results obtained for proline. This is clearly seen in Figure 8 where we show how the relative energies of glycine, alanine, and proline change with the level of theory. Increasing accuracy of the calculations from MP2 to MP4(SDQ) and to CCSD leads to an insignificant decrease of the relative stability of conformer **II**: from 0.4 to

0.6 kJ mol⁻¹ for glycine, from 0.2 to 0.3 kJ mol⁻¹ for alanine, and from 3.5 to 4.0 kJ mol⁻¹ for proline. These changes in the energy do not impact our previous results.^{19,20} The results demonstrate that a more accurate accounting for the electron correlation effects may be needed in some amino acids and related systems.

5. Conclusions

Two proline conformers were identified in the combined matrix-isolation infrared and theoretical ab initio study: the lowest energy conformer with a N···H—O intramolecular H bond and the second conformer with a N—H···O=C H bond. According to the observed integral intensities both conformers are present in the Ar matrix in approximately equal amounts. This is in agreement with the relative energy calculations of the conformers performed at the CCSD and CCSD(T) levels of theory. Both methods predict conformer **IIa** to be the most stable with the energy difference from conformer **Ia** of less than kT at the matrix deposition temperature.

The intramolecular N···H—O H bond in the lowest energy conformer is much stronger than the corresponding H bond in

TABLE 7: Observed and Calculated (at the DFT/B3LYP/aug-cc-pVDZ level) IR Frequencies (cm⁻¹) and Intensities of Proline-d₂

observed ^a			calculated						observed ^a			calculated					
			proline-d ₂ Ia			proline-d ₂ IIa						proline-d ₂ Ia			proline-d ₂ IIa		
ν	A^b	I_{obs}^c	ν	I_{calc}^d	assignment ^e	ν	I_{calc}^d	assignment ^e	ν	A^b	I_{obs}^c	ν	I_{calc}^d	assignment ^e	ν	I_{calc}^d	assignment ^e
2984	0.12	2.66	2992	33.6	C6H str	3008	10.1	C6H str	1059	0.01	0.12	1055	1.5	N1C2C3 bend			
			2980	28.0	C15H str	2990	27.3	C12H str	1038	0.02	0.16				1041	4.4	C2C6 str
2956	0.09	2.11	2971	26.7	C12H str	2961	33.9	C15H str	991	0.15	1.61	1006	35.0	C3O5 str	1004	31.0	OD bend
2934	0.05	0.78	2944	31.4	C6H str	2948	27.8	C2H str	984	0.07	0.32	1003	41.5	OD bend	992	0.9	C12C15 str
2919	0.04	0.83	2924	18.7	C12H str	2935	15.4	C6H str	966	0.01	0.04						
			2923	24.3	C2H str	2930	13.1	C12H str	961	0.01	0.04						
			2898	52.7	C15H str	2884	59.1	C15H str	949	0.01	0.07	952	7.1	C2C6 str			
2884	0.10	2.56							936	0.02	0.13				924	5.2	ring bend
2857	0.02	0.26							927	0.02	0.18	917	1.5	N1C2C3O4 tor	926	6.2	C6C12 str
2840	0.03	0.51							911	0.02	0.31	909	14.1	C6C12 str			
2626	0.13	1.47	2611	45.7	OD str				894	0.05	0.50	894	3.9	C12C15 str	889	15.9	N1C2C3 bend
2617	0.08					2487	5.5	ND str	876	0.03	0.30	871	3.2	ring bend	884	3.5	ND bend
2519	0.01	0.14							858	0.02	0.15				864	7.1	ring bend
2499	0.01	0.22	2458	15.9	ND str				816	0.01	0.14				807	0.9	O4C3C2C6 tor
2295	0.05	5.32				2347	180.2	OD str	763	0.01	0.04	770	5.6	N1C2C3O4 tor			
2248	0.05								754	0.01	0.06				749	2.7	C2C6 str
1779	0.50	6.80				1794	358.5	C=O str	729	0.03	0.33						
1756	0.39	5.99	1766	265.5	C=O str				722	0.02		717	6.1	C2C6 str			
1487	0.01	0.02	1487	0.9	CH bend	1498	0.5	CH bend	690	0.02	0.52	691	61.1	O4C3C2C6 tor	694	7.0	N1C2C3O4 tor
1461	0.02	0.33	1472	2.8	CH bend	1476	7.1	CH bend	672	0.02	0.30						
1452	0.04	0.31	1462	3.5	CH bend	1464	5.6	CH bend	662	0.03	0.19						
1387	0.07	2.39	1378	45.6	C2H bend				656	0.04	0.92						
1344	0.03	0.68	1335	2.6	CH bend	1352	0.3	CH bend	646	0.09					663	33.5	OD tor
1323	0.11	0.76				1327	17.4	CH bend	615	0.04	0.64	613	26.9	ring bend			
1311	0.09	0.46	1316	0.3	CH bend	1315	33.0	C2H bend	604	0.02	0.12						
1301	0.06	0.77							597	0.02	0.18				587	5.3	ring bend
1292	0.07	0.43				1294	3.6	CH bend	589	0.03	0.22	583	14.4	ring bend			
1287	0.06	0.30	1287	7.9	CH bend				579	0.02	0.10						
1281	0.12	0.94							570	0.02	0.16				572	4.1	ring bend
1276	0.07	0.26							555	0.02	0.20	559	11.5	C2C3O4 bend			
1271	0.16	1.06	1267	1.3	CH bend	1279	188.1	C3O5 str	552	0.02							
1257	0.06	1.02	1257	4.8	CH bend	1259	2.2	CH bend	547	0.01							
1238	0.06	0.55				1238	16.6	CH bend	533	0.02	0.09						
1227	0.16	1.92	1218	157.2	C3O5 str				527	0.01	0.56						
1222	0.16								522	0.06					517	27.0	ND tor
1196	0.03	0.22	1196	27.1	CH bend				518	0.02							
1188	0.03	0.20				1180	10.8	CH bend	510	0.03	0.08						
1178	0.05	0.37	1173	2.6	CH bend				450	0.03	0.87	446	43.0	OD tor	454	2.2	C2C3O4 bend
1168	0.08	0.52				1166	27.3	CH bend	430	0.10	0.77	399	14.9	C2C3O5 bend			
1155	0.06	0.81	1145	53.9	N1C2 str				278	4.2	N1C2C3 bend	311	4.9	ring bend			
1139	0.06	0.76							253	1.2	ring tor	278	8.9	C2C3O5 bend			
1123	0.10	1.47				1124	32.9	N1C2 str	191	1.3	ring bend	200	6.5	C2C3C6 bend			
1111	0.03								71	1.3	O4C3C2C6 tor	107	0.5	ring tor			
1100	0.05	0.34	1098	4.2	CH bend	1098	17.1	CH bend	41	1.4	ting tor	55	2.3	O4C3C2C6 tor			
1087	0.02	0.30															

^a Ar matrix deposited at 11 K. Sample-to-matrix ratio 1:500. ^b A, experimental relative intensities. ^c I_{obs} , experimental relative integral intensities measured for the single bands or for the groups of merged bands. ^d I_{calc} , calculated intensities in km mol⁻¹. ^e Abbreviations: str, stretching; bend, bending; tor, torsion.

TABLE 8: Energies (au, First Row) and Relative Stabilities (kJ mol⁻¹, Second Row) of the Lowest Energy Glycine and Alanine Conformers I and II Calculated at the Different Levels of Theory^a

method	I	II
	Glycine	
MP2/6-31++G**//MP2/aug-cc-pVDZ	-283.658646	-283.657801
	0.0	2.2
MP4(sdq)/6-31++G**//MP2/aug-cc-pVDZ	-283.689727	-283.688739
	0.0	2.6
CCSD/6-31++G**//MP2/aug-cc-pVDZ	-283.687728	-283.687728
	0.0	2.8
	Alanine	
MP2/6-31++G**//MP2/aug-cc-pVDZ	-322.857263	-322.855712
	0.0	4.1
MP4(sdq)/6-31++G**//MP2/aug-cc-pVDZ	-322.898151	-322.896502
	0.0	4.3
CCSD/6-31++G**//MP2/aug-cc-pVDZ	-322.896119	-322.894451
	0.0	4.4

^a Relative energies were calculated with respect to the glycine and alanine conformers I.

other amino acids. This stronger H bond makes the proline conformer **IIa** more stable than conformer **Ia**. This is unlike

other amino acids where the **Ia** conformer dominates. The calculated relative stabilities of the proline conformers are

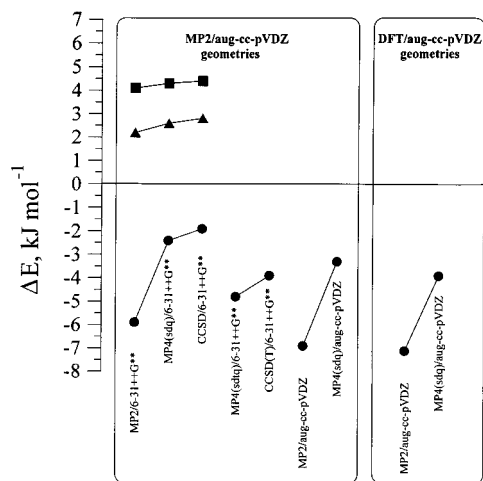


Figure 8. Relative stability of conformer **II** with respect to conformer **I**: (●) proline; (▲) glycine; (■) alanine.

consistent with their IR spectral manifestations. The shifts of the bands in the proline IR spectra due to the N \cdots H–O H bond are stronger in comparison to other amino acids.

The DFT/B3LYP and MP2 methods failed to predict correct relative energies of the two lowest energy proline conformers. Both methods provided too high energy differences and ruled out the presence of conformer **Ia** at the experimental conditions. This was corrected when the CCSD method was applied. Although the relative stabilities of conformers **I** and **II** calculated for several amino acids (glycine, alanine, valine) at the MP2 and DFT levels of theory were in agreement with the CCSD results, this was not the case for proline. Thus the CCSD method should be applied to calculate relative energies in future studies of other amino acids and related systems.

Acknowledgment. This work was supported in part by a NATO grant (CRG.CRG973389) allowing the visit of S.G.S. to the University of Arizona. A partial support from the National Science Foundation is also acknowledged.

References and Notes

- (1) Nemethy, G.; Printz, M. P. *Macromolecules* **1972**, *6*, 755.
- (2) Piela, L.; Nemethy, G.; Scheraga, H. A. *Biopolymers* **1987**, *26*, 1587.
- (3) Choy, P. Y.; Fasman, G. D. *Biochemistry* **1974**, *13*, 211.
- (4) Sankararamkrishnan, R.; Vishveshwara, S. *Biopolymers* **1990**, *30*, 287.
- (5) Dasgupta, S.; Bell, J. A. *J. Peptide Protein Res.* **1993**, *41*, 499.
- (6) Kayushina, R. L.; Vainshtein, K. B. *Sov. Phys. Crystallogr.* **1966**, *10*, 698.
- (7) Brown, R. D.; Godfrey, P. D.; Storey, J. W. V.; Bassez, M. P. *J. Chem. Soc., Chem. Commun.* **1978**, 547.
- (8) Suenram, R. D.; Lovas, F. J. *J. Mol. Spectrosc.* **1978**, *72*, 372.
- (9) (a) Suenram, R. D.; Lovas, F. J. *J. Am. Chem. Soc.* **1980**, *102*, 7180. (b) Schäfer, L.; Sellers, H. L.; Lowas, F. J.; Suenram, R. D. *J. Am.*

Chem. Soc. **1980**, *102*, 6566.

- (10) Iijima, K.; Tanaka, K.; Onuma, S. *J. Mol. Struct.* **1991**, *246*, 257.
- (11) Godfrey, P. D.; Brown, R. D. *J. Am. Chem. Soc.* **1995**, *117*, 2019.
- (12) Lovas, F. J.; Kawashima, Y.; Grabow, J.-U.; Suenram, R. D.; Freser, G. T.; Hirota, E. *Astrophys. J.* **1995**, *455*, 201.
- (13) McGlone, S. J.; Elmes, P. S.; Brown, R. D.; Godfrey, P. D. *J. Mol. Struct.* **1999**, *486*, 225.
- (14) Iijima, K.; Beagley, B. *J. Mol. Struct.* **1991**, *248*, 133.
- (15) Godfrey, P. D.; Firth, S.; Hatherley, L. D.; Brown, R. D.; Pierlot, A. P. *J. Am. Chem. Soc.* **1993**, *115*, 9687.
- (16) Debies, T. P.; Rabalais, J. W. *J. Electron Spectrosc. Relat. Phenom.* **1974**, *3*, 315.
- (17) Klasinc, L. *J. Electron Spectrosc. Relat. Phenom.* **1976**, *8*, 161.
- (18) Reva, I. D.; Plokhotnichenko, A. M.; Stepanian, S. G.; Ivanov, A. Yu.; Radchenko, E. D.; Sheina, G. G.; Blagoi, Yu. P. *Chem. Phys. Lett.* **1995**, *232*, 141. Erratum. *Chem. Phys. Lett.* **1995**, *235*, 617.
- (19) Stepanian, S. G.; Reva, I. D.; Rosado, M. T. S.; Duarte, M. L. T. S.; Fausto, R.; Radchenko, E. D.; Adamowicz, L. *J. Phys. Chem. A* **1998**, *102*, No. 2, 1041.
- (20) Stepanian, S. G.; Reva, I. D.; Radchenko, E. D.; Adamowicz, L. *J. Phys. Chem. A* **1998**, *102*, No. 2, 4623.
- (21) Stepanian, S. G.; Reva, I. D.; Radchenko, E. D.; Adamowicz, L. *J. Phys. Chem. A* **1999**, *103*, No. 3, 4404.
- (22) Sapse, A.-M.; Mallah-Levy, L.; Daniels, S. B.; Ericson, J. *J. Am. Chem. Soc.* **1987**, *109*, 3526.
- (23) Tarakeshwar, P.; Manogaran, S. *J. Mol. Struct. (THEOCHEM)* **1996**, *365*, 167.
- (24) Ramek, M.; Kelterer, A.-M.; Nikolic, S. *Int. J. Quantum Chem.* **1997**, *65*, 1033.
- (25) Csaszar, A. G.; Perczel, A. *Prog. Biophys. Mol. Biol.* **1999**, *71*, 243.
- (26) Reva, I. D.; Stepanian, S. G.; Plokhotnichenko, A. M.; Radchenko, E. D.; Sheina, G. G.; Blagoi, Yu. P. *J. Mol. Struct.* **1994**, *318*, 1.
- (27) Radchenko, E. D.; Sheina, G. G.; Smorygo N. A.; Blagoi Yu. P. *J. Mol. Struct.* **1984**, *116*, 387.
- (28) Becke, A. D. *Phys. Rev. B* **1988**, *38*, 3098.
- (29) Lee, C.; Yang, W.; Parr, R. G. *Phys. Rev. B* **1988**, *37*, 785.
- (30) Vosko, S. H.; Wilk, L.; Nusair, M. *Can. J. Phys.* **1980**, *58*, 1200.
- (31) Krishmah, R.; Pople, J. A. *Int. J. Quantum Chem.* **1978**, *14*, 91.
- (32) Krishmah, R.; Frisch, M. J.; Pople, J. A. *J. Chem. Phys.* **1980**, *72*, 4244.
- (33) Cizek, J. *Adv. Chem. Rev.* **1969**, *14*, 35.
- (34) Purvis, G. D.; Bartlett, R. J. *J. Chem. Phys.* **1982**, *76*, 1910.
- (35) Scuseria, G. E.; Janssen, C. L.; Schaefer, H. F., III. *J. Chem. Phys.* **1988**, *89*, 7382.
- (36) Scuseria, G. E.; Schaefer, H. F., III. *J. Chem. Phys.* **1989**, *90*, 3700.
- (37) Frisch, M. J.; Trucks, G. W.; Schlegel, H. B.; Scuseria, G. E.; Robb, M. A.; Cheeseman, J. R.; Zakrzewski, V. G.; Montgomery, J. A., Jr.; Stratmann, R. E.; Burant, J. C.; Dapprich, S.; Millam, J. M.; Daniels, A. D.; Kudin, K. N.; Strain, M. C.; Farkas, O.; Tomasi, J.; Barone, V.; Cossi, M.; Cammi, R.; Mennucci, B.; Pomelli, C.; Adamo, C.; Clifford, S.; Ochterski, J.; Petersson, G. A.; Ayala, P. Y.; Cui, Q.; Morokuma, K.; Malick, D. K.; Rabuck, A. D.; Raghavachari, K.; Foresman, J. B.; Cioslowski, J.; Ortiz, J. V.; Baboul, A. G.; Stefanov, B. B.; Liu, G.; Liashenko, A.; Piskorz, P.; Komaromi, I.; Gomperts, R.; Martin, R. L.; Fox, D. J.; Keith, T.; Al-Laham, M. A.; Peng, C. Y.; Nanayakkara, A.; Gonzalez, C.; Challacombe, M.; Gill, P. M. W.; Johnson, B.; Chen, W.; Wong, M. W.; Andres, J. L.; Gonzalez, C.; Head-Gordon, M.; Replogle, E. S.; Pople, J. A. *Gaussian 98*, Revision A.7; Gaussian, Inc.: Pittsburgh, PA, 1998.
- (38) Stepanian, S. G.; Reva, I. D.; Radchenko, E. D.; Sheina, G. G.; Blagoi, Yu. P. *Vibr. Spectrosc.* **1996**, *11*, 123.
- (39) Plokhotnichenko, A. M.; Ivanov, A. Yu.; Radchenko, E. D.; Sheina, G. G.; Blagoi, Yu. P. *Low Temp. Phys.* **1993**, *19*, 732.
- (40) Stepanian, S. G.; Reva, I. D.; Kononov, A. Yu.; Adamowicz, L. *J. Phys. Chem.* **2001**, in preparation.